Journal of Sound and Vibration 329 (2010) 1191–1207

Contents lists available at ScienceDirect

Journal of Sound and Vibration

journal homepage: www.elsevier.com/locate/jsvi

Exact transient vibration of stepped bars, shafts and strings carrying lumped masses

Bingen Yang *

Department of Aerospace and Mechanical Engineering, University of Southern California, 3650 McClintock Avenue, Room 430, Los Angeles, CA 90089-1453, USA

ARTICLE INFO

Article history:
Received 23 October 2008
Received in revised form
21 September 2009
Accepted 27 October 2009
Handling Editor: C.L. Morfey
Available online 3 December 2009

ABSTRACT

A new analytical method is developed for transient vibration analysis of stepped systems composed of distributed components like elastic bars, flexible shafts and taut strings, and lumped masses. The method, with a distributed transfer function formulation and a residue formula for inverse Laplace transform, gives the exact transient response of a stepped system with any number of components and subject to arbitrary external, boundary and initial excitations. The proposed method does not depend on system eigenfunctions, is able to accurately predict jumps in stress and strain distributions, and is numerically efficient as its utility only requires simple operations of two-by-two matrices.

1. Introduction

Vibration of stepped distributed dynamic systems is important in many engineering applications, such as buildings, bridges, rotating machines, turbines, helicopters and aerospace structures, and hence has been extensively studied [1–3]. This paper is concerned with stepped systems that are assemblages of one-dimensional distributed components (like elastic bars, torsional shafts and taut strings), and lumped masses. Previous investigations on this type of vibrating systems have been focused on free vibration, forced response to sinusoidal excitations and wave propagation, and analytical solutions have been derived for these problems [4–9]. Determination of transient vibration of stepped distributed systems, however, has mainly replied on numerical methods, although certain analytical results can be obtained by eigenfunction expansion [10–12], and by a time-domain receptence method that is valid for stepped systems with lumped parameter components [13,14].

There are several issues that restrict the utility of the existing analytical techniques in transient analysis of stepped systems. First, conventional eigenfunction expansion or modal analysis, while being able to give transient solutions of stepped systems under external loads, is not directly applicable to stepped systems subject to boundary excitations, settlement of foundation, and motions of spring constraint supports. Handling these inhomogeneous terms in the boundary and matching conditions is not trivial in a modal analysis. Second, in transient analysis Laplace transform method and transfer matrix method are crippled by complicated s-domain expressions whose inverse Laplace transforms have to be found. In fact, exact transient solutions via inverse Laplace transform become difficult if a stepped system with three or more distributed components is considered. Third, solution by most analytical techniques is problem-dependent, requesting different derivations and algorithms for different system configurations (number of components, boundary

* Tel.: +1 213 740 7082.
E-mail address: bingen@usc.edu

0022-460X/$ - see front matter © 2009 Elsevier Ltd. All rights reserved.
doi:10.1016/j.jsv.2009.10.035

conditions, constraints and lumped masses, etc.). This inflexibility in treating stepped systems makes analytical techniques less user-friendly, compared to numerical methods, such as the finite element method.

In this work, a new analytical technique is developed for exact solution of transient vibration problems of stepped distributed systems. By exact solution, we mean that the response of a stepped distributed system can be expressed by an infinite series, with each term individually determined in exact and closed form. The new technique is an extension of the distributed transfer function method (DTFM) [15–18]. The DTFM was developed for vibration analysis and feedback control of elastic continua, but it has not been applied to transient vibration problems of stepped systems. The proposed DTFM is capable of obtaining exact transient solutions for a stepped system with any number of components and arbitrary boundary conditions, and at the same time avoids the aforementioned issues of the existing analytical techniques. The DTFM, with a spatial state formulation and a formula for evaluation of transfer function residues, obtains transient solutions in a symbolic manner. As shall be seen, this new method is numerically efficient because its utility only involves simple operations of two-by-two matrices.

The remainder of the paper is arranged as follows. The vibration problem of stepped distributed systems is described in Section 2. A distributed transfer function formulation is derived in Section 3, and based on this formulation system eigensolutions are determined in Sections 4. In Section 5, a Green's function integral and a formula for precise evaluation of transfer function residues are obtained which eventually leads to exact transient solutions of stepped systems. The proposed method is illustrated on two examples in Section 6.

2. Statement of problem

The stepped distributed system in consideration is an assembly of n one-dimensional, serially connected, elastic components; see Fig. 1, where x_i, $i=1,2,\ldots,n-1$, are the interior nodes at which adjacent components are interconnected, x_0 and x_n are the boundary nodes representing the ends of the system, and $l_i=x_{i+1}-x_i$ is the length of the ith component. Set $x_0=0$, so that $x_i=l_1+l_2+\cdots+l_i$ for $i=1,2,\ldots,n$. The vibration of the ith component is governed by the wave equation

$$\rho_i\frac{\partial^2 w_i(x,t)}{\partial t^2}-\alpha_i^{ST}\frac{\partial^2 w_i(x,t)}{\partial x^2}=f_i(x,t),\quad x\in(x_{i-1},x_i) \tag{1}$$

where $w_i(x,t)$ is the displacement of the component, ρ_i an inertia parameter, α_i^{ST} a stiffness parameter, and $f_i(x,t)$ an external load. Eq. (1) is a model for elastic bars in longitudinal vibration, circular shafts in torsional vibration, and taut strings in transverse vibration; see Table 1 for the physical meaning of related parameters. At the nodes of the stepped system there may be spring constrains and mounted lumped masses. The interface between the ith and $(i+1)$th components at node x_i is described by the matching conditions

$$w_i(x_i,t)=w_{i+1}(x_i,t)$$

$$m_i\frac{\partial^2 w_i(x_i,t)}{\partial t^2}+\alpha_i^{ST}\frac{\partial w_i(x_i,t)}{\partial x}+k_iw_i(x_i,t)=\alpha_{i+1}^{ST}\frac{\partial w_{i+1}(x_i,t)}{\partial x}+q_i(t)+k_iz_i(t) \tag{2}$$

for $i=1,2,\ldots,n-1$, where m_i is a lumped mass or a rigid disk, k_i the coefficient of a spring; $q_i(t)$ an external force load applied at the lumped mass, and $z_i(t)$ a foundation motion of the node. The boundary conditions of the stepped system are of the general form

$$\text{at } x=x_0:\quad m_L\frac{\partial^2 w_1}{\partial t^2}+a_1\frac{\partial w_1}{\partial x}+a_0w_1=\gamma_L(t)$$

$$\text{at } x=x_n:\quad m_R\frac{\partial^2 w_n}{\partial t^2}+b_1\frac{\partial w_n}{\partial x}+b_0w_n=\gamma_R(t) \tag{3}$$

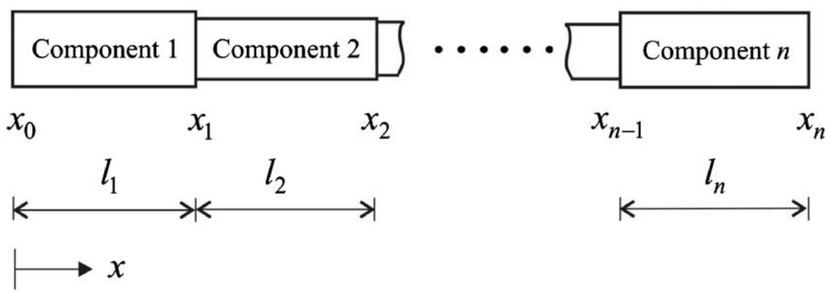

Fig. 1. Schematic of an n-component stepped distributed dynamic system.

Table 1
Parameters of distributed components.

	Displacement $w(x, t)$	Inertia parameter ρ	Stiffness parameter α^{ST}
Elastic bar	Longitudinal displacement $u(x, t)$	Linear density $\rho_v A$	Longitudinal rigidity EA
Circular shaft	Rotation (twist) $\theta(x, t)$	Polar mass moment of inertia $\rho_v J$	Torsional rigidity GJ
Taut string	Transverse displacement $y(x, t)$	Linear density $\rho_v A$	Tension T

ρ_v—mass per unit volume, A—cross-section area, J—moment of inertia.

where a_0, a_1, b_0 and b_1 are constants that are properly assigned to characterize different types of boundaries; m_L and m_R are end masses; and $\gamma_L(t)$ and $\gamma_R(t)$ are related to prescribed boundary excitations (external load or possible foundation motion). In addition, the system is subject to the initial conditions

$$w_i(x,0) = u_{0,i}(x), \quad \frac{\partial w_i(x,0)}{\partial t} = v_{0,i}(x), \quad x \in (x_{i-1}, x_i) \tag{4}$$

for $i = 1, 2, \ldots, n$, where $u_{0,i}(x)$ and $v_{0,i}(x)$ are given profiles of initial displacement and velocity of the ith component.

In this work, we shall obtain analytical solutions of the boundary-initial value problem formed by Eqs. (1)–(4). A Laplace transform method is developed to obtain exact transient response of the stepped system subject to arbitrary external loads, boundary excitations, and initial disturbances.

3. Distributed transfer function formulation

The s-domain solution of the stepped distributed system is first devised by the distributed transfer function method [15–18]. To this end, take Laplace transform of Eqs. (1)–(3) with respect to time, which gives

$$\frac{\partial^2 \overline{w}_i(x,s)}{\partial x^2} = \frac{s^2}{c_i^2}\overline{w}_i(x,s) - \frac{1}{\alpha_i^{ST}}(\overline{f}_i(x,s) + s u_{0,i}(x) + v_{0,i}(x)), \quad x \in (x_{i-1}, x_i) \tag{5}$$

for $i = 1, 2, \ldots, n$,

$$\overline{w}_{i+1}(x_i, s) = \overline{w}_i(x_i, s)$$

$$\alpha_{i+1}^{ST}\frac{\partial \overline{w}_{i+1}(x_i,s)}{\partial x} = \alpha_i^{ST}\frac{\partial \overline{w}_i(x_i,s)}{\partial x} + (m_i s^2 + k_i)\overline{w}_i(x_i,s) - \hat{q}_{e0,i}(s) \tag{6a}$$

for $1 \le i \le n-1$, and

$$a_1\frac{\partial \overline{w}_1(x_0,s)}{\partial x} + (m_L s^2 + a_0)\overline{w}_1(x_0,s) = \overline{\gamma}_L(s) + m_L(s u_{0,1}(x_0) + v_{0,1}(x_0))$$

$$b_1\frac{\partial \overline{w}_n(x_n,s)}{\partial x} + (m_R s^2 + b_0)\overline{w}_n(x_n,s) = \overline{\gamma}_R(s) + m_R(s u_{0,n}(x_n) + v_{0,n}(x_n)) \tag{6b}$$

where the over-bar stands for Laplace transform, s is the Laplace transform parameter, $c_i = \sqrt{\alpha_i^{ST}/\rho_i}$, and

$$\hat{q}_{e0,i}(s) = \overline{q}_i(s) + k_i\overline{z}_i(s) + m_i(s u_{0,i}(x_i) + v_{0,i}(x_i)) \tag{7}$$

The initial conditions (4) are embedded in Eqs. (5) and (6). By defining the spatial state vector

$$\hat{\boldsymbol{\eta}}_i(x,s) = \begin{pmatrix} \overline{w}_i(x,s) \\ \dfrac{\partial \overline{w}_i(x,s)}{\partial x} \end{pmatrix}, \quad x \in (x_{i-1}, x_i) \tag{8}$$

Eq. (5) is rewritten in a first-order state form

$$\frac{\partial}{\partial x}\hat{\boldsymbol{\eta}}_i(x,s) = \boldsymbol{F}_i(s)\hat{\boldsymbol{\eta}}_i(x,s) + \hat{\boldsymbol{p}}_i(x,s), \quad x \in (x_{i-1}, x_i), \ \ i = 1, 2, \ldots, n \tag{9}$$

where

$$\boldsymbol{F}_i(s) = \begin{bmatrix} 0 & 1 \\ s^2/c_i^2 & 0 \end{bmatrix}, \quad \hat{\boldsymbol{p}}_i(x,s) = -\frac{1}{\alpha_i^{ST}}(\overline{f}_i(x,s) + s\rho_i u_{0,i}(x) + \rho_i v_{0,i}(x))\begin{pmatrix} 0 \\ 1 \end{pmatrix} \tag{10}$$

For convenience of analysis, define a global domain $\Omega = (x_0, x_1) \cup (x_1, x_2) \cup \cdots \cup (x_{n-1}, x_n)$ and convert Eq. (9) to a global state equation

$$\frac{\partial}{\partial x}\hat{\boldsymbol{\eta}}(x,s) = \boldsymbol{F}(x,s)\hat{\boldsymbol{\eta}}(x,s) + \hat{\boldsymbol{p}}(x,s), \quad x \in \Omega \tag{11}$$

where the global quantities

$$\hat{\boldsymbol{\eta}}(x,s)=\hat{\boldsymbol{\eta}}_i(x,s),\quad \boldsymbol{F}(x,s)=\boldsymbol{F}_i(s),\quad \hat{\boldsymbol{p}}(x,s)=\hat{\boldsymbol{p}}_i(x,s) \tag{12}$$

for $x\in(x_{i-1},x_i)$, $i=1,2,\ldots,n$. The matching and boundary conditions (6) are also cast into a global state form

$$\hat{\boldsymbol{\eta}}(x_i+,s)=\boldsymbol{T}_i\hat{\boldsymbol{\eta}}(x_i-,s)-\boldsymbol{\nu}_i(s),\quad i=1,2,\ldots,n-1 \tag{13}$$

$$\boldsymbol{M_b}\hat{\boldsymbol{\eta}}(x_0,s)+\boldsymbol{N_b}\hat{\boldsymbol{\eta}}(x_n,s)=\boldsymbol{\gamma_b}(s) \tag{14}$$

where

$$\boldsymbol{T}_i=\begin{bmatrix}1 & 0\\ \dfrac{m_is^2+k_i}{\alpha_{i+1}^{ST}} & \dfrac{\alpha_i^{ST}}{\alpha_{i+1}^{ST}}\end{bmatrix},\quad \boldsymbol{\nu}_i(s)=\frac{1}{\alpha_{i+1}^{ST}}\hat{q}_{e0,i}(s)\begin{pmatrix}0\\1\end{pmatrix}$$

$$\boldsymbol{M_b}=\begin{bmatrix}m_Ls^2+a_0 & a_1\\ 0 & 0\end{bmatrix},\quad \boldsymbol{N_b}=\begin{bmatrix}0 & 0\\ m_Rs^2+b_0 & b_1\end{bmatrix}$$

$$\boldsymbol{\gamma_b}(s)=\begin{pmatrix}\overline{\gamma}_L(s)\\ \overline{\gamma}_R(s)\end{pmatrix}+\begin{pmatrix}m_L(su_{0,1}(x_0)+v_{0,1}(x_0))\\ m_R(su_{0,n}(x_n)+v_{0,n}(x_n))\end{pmatrix} \tag{15}$$

Hence, the s-domain response of the stepped system is governed by the global state Eq. (11), along with the matching conditions (13) and boundary condition (14).

In this study, the state Eq. (11) is solved through use of state transition matrix. The state transition matrix of the stepped system is the unique solution of [19]

$$\frac{\partial}{\partial x}\boldsymbol{\Phi}(x,\xi,s)=\boldsymbol{F}(x,s)\boldsymbol{\Phi}(x,\xi,s),\quad x,\xi\in\Omega \tag{16}$$

that satisfies conditions

$$\boldsymbol{\Phi}(x,x,s)=\boldsymbol{I}$$

$$\boldsymbol{\Phi}(x_i+,\xi,s)=\boldsymbol{T}_i\boldsymbol{\Phi}(x_i-,\xi,s),\quad \xi\in\Omega,\ \ i=1,2,\ldots,n-1 \tag{17}$$

where $\boldsymbol{I}$ is the identity matrix. The state transition matrix has the properties

$$\boldsymbol{\Phi}^{-1}(x,\xi,s)=\boldsymbol{\Phi}(\xi,x,s)$$

$$\boldsymbol{\Phi}(x,z,s)=\boldsymbol{\Phi}(x,y,s)\boldsymbol{\Phi}(y,z,s) \tag{18}$$

Furthermore, the state transition matrix can be written as

$$\boldsymbol{\Phi}(x,\xi,s)=\boldsymbol{U}(x,s)\boldsymbol{U}^{-1}(\xi,s) \tag{19}$$

where $\boldsymbol{U}(x,s)$ is any fundamental matrix that is a nonsingular solution of

$$\frac{\partial}{\partial x}\boldsymbol{U}(x,s)=\boldsymbol{F}(x,s)\boldsymbol{U}(x,s),\quad x\in\Omega \tag{20}$$

subject to the condition $\boldsymbol{U}(x_i+,s)=\boldsymbol{T}_i\boldsymbol{U}(x_i-,s)$, $i=1,2,\ldots,n-1$. It can be shown that a fundamental matrix for the stepped system is

$$\boldsymbol{U}(x,s)=\begin{cases}e^{\boldsymbol{F}_1(s)(x-x_0)}, & x\in(x_0,x_1)\\ e^{\boldsymbol{F}_i(s)(x-x_{i-1})}\boldsymbol{T}_{i-1}e^{\boldsymbol{F}_{i-1}(s)l_{i-1}}\cdots\boldsymbol{T}_1e^{\boldsymbol{F}_1(s)l_1}, & x\in(x_{i-1},x_i),\ \ 2\le i\le n\end{cases} \tag{21}$$

where $e^{\boldsymbol{F}_i(s)x}$ are exponential matrices [19], and from Eq. (9) they are derived as

$$e^{\boldsymbol{F}_i(s)x}=\begin{bmatrix}\cosh\left(\dfrac{s}{c_i}x\right) & \dfrac{c_i}{s}\sinh\left(\dfrac{s}{c_i}x\right)\\ \dfrac{s}{c_i}\sinh\left(\dfrac{s}{c_i}x\right) & \cosh\left(\dfrac{s}{c_i}x\right)\end{bmatrix} \tag{22}$$

By Eq. (21), $\boldsymbol{U}$=(x_0, s)=$\boldsymbol{I}$, and as a result

$$\boldsymbol{\Phi}(x,x_0,s)=\boldsymbol{U}(x,s) \tag{23}$$

With the state transition matrix given in Eqs. (19) and (21), the s-domain response of the stepped system is taken as

$$\hat{\boldsymbol{\eta}}(x,s)=\int_{x_0}^{x_n}\hat{\boldsymbol{G}}(x,\xi,s)\hat{\boldsymbol{p}}(\xi,s)\,d\xi+\hat{\boldsymbol{H}}(x,s)\boldsymbol{\gamma_b}(s)-\sum_{i=1}^{n-1}\hat{\boldsymbol{G}}(x,x_i+,s)\boldsymbol{\nu}_i(s) \tag{24}$$

where

$$\hat{\boldsymbol{G}}(x,\xi,s)=\begin{cases}\hat{\boldsymbol{H}}(x,s)\boldsymbol{M_b}\boldsymbol{\Phi}(x_0,\xi,s), & \xi\le x\\ -\hat{\boldsymbol{H}}(x,s)\boldsymbol{N_b}\boldsymbol{\Phi}(x_n,\xi,s), & \xi>x\end{cases} \tag{25}$$

$$\hat{\boldsymbol{H}}(x,s)=\boldsymbol{\Phi}(x,x_0,s)\boldsymbol{Z}^{-1}(s)$$

with

$$\boldsymbol{Z}(s)=\boldsymbol{M_b}+\boldsymbol{N_b}\boldsymbol{\Phi}(x_n,x_0,s) \tag{26}$$

The matrices $\hat{\boldsymbol{G}}$ and $\hat{\boldsymbol{H}}$ are called the distributed transfer functions of the stepped system, and $\boldsymbol{Z}(s)$ the boundary impedance matrix. See Appendix A for the proof of Eq. (24).

The spatial state Eq. (11) and the transfer function formulation (24) lay out a foundation for determination of the eigensolutions and transient response of the stepped system, as shall be seen in the subsequent sections.

4. Eigensolutions

Define the eigenvalue problem of the stepped distributed system by vanishing the excitation terms in Eqs. (11), (13) and (14):

$$\frac{\partial}{\partial x}\boldsymbol{\psi}(x)=\boldsymbol{F}(x,s)\boldsymbol{\psi}(x),\quad x\in\Omega \tag{27}$$

subject to the conditions

$$\boldsymbol{\psi}(x_i+)=\boldsymbol{T}_i\boldsymbol{\psi}(x_i-),\quad i=1,2,\ldots,n-1 \tag{28a}$$

$$\boldsymbol{M_b}\boldsymbol{\psi}(x_0)+\boldsymbol{N_b}\boldsymbol{\psi}(x_n)=0 \tag{28b}$$

where s is an eigenvalue, and $\boldsymbol{\psi}(x)$ the eigenfunction associated with s. Write

$$\boldsymbol{\psi}(x)=\boldsymbol{\Phi}(x,x_0,s)\boldsymbol{a} \tag{29}$$

with $\boldsymbol{a}$ being a vector to be determined, which satisfies Eqs. (27) and (28a). Plugging Eq. (29) into the boundary condition (28b) gives

$$(\boldsymbol{M_b}+\boldsymbol{N_b}\boldsymbol{\Phi}(x_n,x_0,s))\boldsymbol{a}=0 \tag{30}$$

The characteristic equation of the stepped system then is

$$\det\boldsymbol{Z}(s)=\det(\boldsymbol{M_b}+\boldsymbol{N_b}\boldsymbol{\Phi}(x_n,x_0,s))=0 \tag{31}$$

The roots of Eq. (31) can be written as $s_k=\mathrm{j}\omega_k$, $\mathrm{j}=\sqrt{-1}$, $k=1,2,\ldots$, where ω_k is the kth natural frequency of the system. From Eqs. (31) and (23), the natural frequencies are the nonnegative roots of the real-valued transcendental equation

$$\Delta(\omega)\equiv\det(\boldsymbol{M_b}+\boldsymbol{N_b}\boldsymbol{W}(\omega))=0 \tag{32}$$

where

$$\boldsymbol{W}(\omega)\equiv\boldsymbol{U}(x_n,\mathrm{j}\omega)=\mathrm{e}^{\boldsymbol{F}_n(\mathrm{j}\omega)l_n}\boldsymbol{T}_{n-1}\mathrm{e}^{\boldsymbol{F}_{n-1}(\mathrm{j}\omega)l_{n-1}}\cdots\boldsymbol{T}_1\mathrm{e}^{\boldsymbol{F}_1(\mathrm{j}\omega)l_1} \tag{33}$$

with

$$\mathrm{e}^{\boldsymbol{F}_i(\mathrm{j}\omega)x}=\begin{bmatrix}\cos\left(\dfrac{\omega}{c_i}x\right) & \dfrac{c_i}{\omega}\sin\left(\dfrac{\omega}{c_i}x\right)\\ -\dfrac{\omega}{c_i}\sin\left(\dfrac{\omega}{c_i}x\right) & \cos\left(\dfrac{\omega}{c_i}x\right)\end{bmatrix},\quad i=1,2,\ldots,n \tag{34}$$

The characteristic function $\Delta(\omega)$ has the following two properties:

(i) The function is finite at $\omega=0$

$$\Delta(0)=\det\left(\boldsymbol{M_b}+\boldsymbol{N_b}\begin{bmatrix}1 & l_n\\ 0 & 1\end{bmatrix}\boldsymbol{T}_{n-1}\begin{bmatrix}1 & l_{n-1}\\ 0 & 1\end{bmatrix}\ldots\boldsymbol{T}_1\begin{bmatrix}1 & l_1\\ 0 & 1\end{bmatrix}\right) \tag{35}$$

(ii) For the stepped system carrying m lumped masses $(0\le m\le n+1)$

$$\Delta(\omega)=\sum_{j=-n_2}^{n_1}\omega^j\phi_j(\omega) \tag{36}$$

where $0\le n_1\le m+1$, $n_2\ge 1$, and $\phi_j(\omega)$ are functions that only contain sinusoidal components like $\sin(\omega l_i/c_i)$ and $\cos(\omega l_i/c_i)$.

According to these properties, $\Delta(\omega)$ is well-behaved. With proper scaling, such as $\Delta(\omega)/(1+\omega^{n_1})$, the function is bounded for any $\omega\geq 0$. Therefore, standard root-searching techniques are directly applicable to Eq. (32) for accurate eigenvalue solutions.

Although eigenfunctions are not needed in the proposed transient analysis, they are useful in free vibration analysis. The eigenfunction (mode shape) associated with $\mathrm{j}\omega_k$ is given by

$$\boldsymbol{\psi}_k(x)=\boldsymbol{\Phi}(x,x_0,\mathrm{j}\omega_k)\boldsymbol{a}_k \tag{37}$$

where $\boldsymbol{a}_k$ is a nonzero solution of the homogeneous equation $\boldsymbol{Z}(\mathrm{j}\omega_k)\boldsymbol{a}=0$.

5. Transient response

In this study, exact transient solutions are obtained by the distributed transfer function formulation obtained in Section 3 and by a new residue formula for inverse Laplace transform.

5.1. Green's function formula

Inverse Laplace transform of Eq. (24) yields Green's function formula

$$\begin{aligned}\boldsymbol{\eta}(x,t)= &-\sum_{i=1}^{n}\frac{1}{\alpha_i^{ST}}\int_0^t\int_{x_{i-1}}^{x_i}\boldsymbol{G}(x,\xi,t-\tau)f_i(\xi,\tau)\,\mathrm{d}\xi\,\mathrm{d}\tau\begin{pmatrix}0\\1\end{pmatrix}-\sum_{i=1}^{n-1}\frac{1}{\alpha_i^{ST}}\int_0^t\boldsymbol{G}(x,x_i+,\tau)(q_i(\tau)+k_iz_i(\tau))\,\mathrm{d}\tau\begin{pmatrix}0\\1\end{pmatrix}\\ &+\int_0^t\boldsymbol{H}(x,t-\tau)\begin{pmatrix}\gamma_L(t)\\\gamma_R(t)\end{pmatrix}\mathrm{d}\tau-\sum_{i=1}^{n}\frac{\rho_i}{\alpha_i^{ST}}\int_{x_{i-1}}^{x_i}\left(\frac{\partial}{\partial t}\boldsymbol{G}(x,\xi,t)u_{0,i}(\xi)+\boldsymbol{G}(x,\xi,t)v_{0,i}(\xi)\right)\mathrm{d}\xi\begin{pmatrix}0\\1\end{pmatrix}\\ &-\sum_{i=1}^{n-1}\frac{m_i}{\alpha_{i+1}^{ST}}\left(\frac{\partial}{\partial t}\boldsymbol{G}(x,x_i+,t)u_{0,i}(x_i)+\boldsymbol{G}(x,x_i+,t)v_{0,i}(x_i)\right)\begin{pmatrix}0\\1\end{pmatrix}\\ &+\frac{\partial}{\partial t}\boldsymbol{H}(x,t)\begin{pmatrix}m_Lu_{0,1}(x_0)\\m_Ru_{0,n}(x_n)\end{pmatrix}+\boldsymbol{H}(x,t)\begin{pmatrix}m_Lv_{0,1}(x_0)\\m_Rv_{0,n}(x_n)\end{pmatrix}\end{aligned} \tag{38}$$

for $x\in\Omega$, where $\boldsymbol{\eta}(x,t)$ is the inverse Laplace transform of $\hat{\boldsymbol{\eta}}(x,s)$; and the matrix Green's functions $\boldsymbol{G}$ and $\boldsymbol{H}$ are the inverse Laplace transforms of the transfer functions $\hat{\boldsymbol{G}}$ and $\hat{\boldsymbol{H}}$, respectively. The first four terms on the right-hand side of Eq. (38) represent the effects of external loads, boundary excitations and initial disturbances, and determination of the transient response of a stepped distributed system are the contributions of the lumped masses due to the initial disturbances. According to Eqs. (25), (26) and (31), the distributed transfer functions have an infinite number of poles, $\pm\mathrm{j}\omega_k$, $k=1,2,\ldots$ By the theorem of residues [20], Green's functions are of the form

$$\boldsymbol{G}(x,\xi,t)=\sum_{k=1}^{\infty}\{\boldsymbol{U}(x,\mathrm{j}\omega_k)\boldsymbol{R}_k\boldsymbol{D}(x,\xi,\mathrm{j}\omega_k)\mathrm{e}^{\mathrm{j}\omega_kt}+\boldsymbol{U}(x,-\mathrm{j}\omega_k)\boldsymbol{R}_{-k}\boldsymbol{D}(x,\xi,-\mathrm{j}\omega_k)\mathrm{e}^{-\mathrm{j}\omega_kt}\} \tag{39a}$$

$$\boldsymbol{H}(x,t)=\sum_{k=1}^{\infty}\{\boldsymbol{U}(x,\mathrm{j}\omega_k)\boldsymbol{R}_k\mathrm{e}^{\mathrm{j}\omega_kt}+\boldsymbol{U}(x,-\mathrm{j}\omega_k)\boldsymbol{R}_{-k}\mathrm{e}^{-\mathrm{j}\omega_kt}\} \tag{39b}$$

where

$$\boldsymbol{D}(x,\xi,s)=\begin{cases}\boldsymbol{M_b}\boldsymbol{\Phi}(x_0,\xi,s), & \xi\leq x\\ -\boldsymbol{N_b}\boldsymbol{\Phi}(x_n,\xi,s), & \xi>x\end{cases} \tag{40}$$

and Eq. (23) has been used. The matrices $\boldsymbol{R}_k$ and $\boldsymbol{R}_{-k}$, which shall be called the residues of the distributed transfer functions, are defined as

$$\boldsymbol{R}_{\pm k}=\operatorname*{Res}_{s=\pm\mathrm{j}\omega_k}(\boldsymbol{Z}(s)^{-1}) \tag{41}$$

The transient response of the stepped distributed system can be determined by Eq. (38) if the transfer function residues are known.

5.2. Transfer function residues

The transfer function residues can be expressed as [20]

$$\boldsymbol{R}_{\pm k}=\frac{\operatorname{adj}\boldsymbol{Z}(\pm\mathrm{j}\omega_k)}{\frac{\mathrm{d}}{\mathrm{d}s}|\boldsymbol{Z}(s)|_{s=\pm\mathrm{j}\omega_k}} \tag{42}$$

where adj$\boldsymbol{Z}(s)$ and $|\boldsymbol{Z}(s)|$ are the adjoint and determinant of $\boldsymbol{Z}(s)$. As shown in Appendix B:

$$\frac{\mathrm{d}}{\mathrm{d}s}|\boldsymbol{Z}(s)|_{s=\pm \mathrm{j}\omega_k} = \pm \mathrm{j} Z_D(\omega_k) \tag{43}$$

where $Z_D(\omega_k)$ is a real number given by

$$Z_D(\omega_k) = \det(\boldsymbol{M}_k + \boldsymbol{N}_k \boldsymbol{d}_W(\omega_k)) + \det(\boldsymbol{d}_{M,k} + \boldsymbol{N}_k \boldsymbol{W}(\omega_k)) + \det(\boldsymbol{M}_k + \boldsymbol{d}_{N,k}\boldsymbol{W}(\omega_k)) \tag{44}$$

Here $\boldsymbol{W}(\omega_k)$ is given in Eq. (33), and

$$\boldsymbol{M}_k = \begin{bmatrix} -m_L\omega_k^2 + a_0 & a_1 \\ 0 & 0 \end{bmatrix}, \quad \boldsymbol{N}_k = \begin{bmatrix} 0 & 0 \\ -m_R\omega_k^2 + b_0 & b_1 \end{bmatrix}$$

$$\boldsymbol{d}_{M,k} = \begin{bmatrix} 2m_L\omega_k & 0 \\ 0 & 0 \end{bmatrix}, \quad \boldsymbol{d}_{N,k} = \begin{bmatrix} 0 & 0 \\ 2m_R\omega_k & 0 \end{bmatrix} \tag{45}$$

$$\begin{aligned}\boldsymbol{d}_W(\omega_k) = {}& \boldsymbol{E}_n(\omega_k)\boldsymbol{T}_{n-1}(\omega_k)\mathrm{e}^{\boldsymbol{F}_{n-1}(\mathrm{j}\omega_k)l_{n-1}} \cdots \boldsymbol{T}_1(\omega_k)\mathrm{e}^{[\boldsymbol{F}_1(\mathrm{j}\omega_k)]l_1} + \mathrm{e}^{\boldsymbol{F}_n(\mathrm{j}\omega_k)l_n}\boldsymbol{\delta T}_{n-1}(\omega_k)\mathrm{e}^{\boldsymbol{F}_{n-1}(\mathrm{j}\omega_k)l_{n-1}} \cdots \boldsymbol{T}_1(\omega_k)\mathrm{e}^{\boldsymbol{F}_1(\mathrm{j}\omega_k)l_1} \\ & + \cdots + \mathrm{e}^{\boldsymbol{F}_n(\mathrm{j}\omega_k)l_n}\boldsymbol{T}_{n-1}(\omega_k)\mathrm{e}^{\boldsymbol{F}_{n-1}(\mathrm{j}\omega_k)l_{n-1}} \cdots \boldsymbol{T}_1(\omega_k)\boldsymbol{E}_1(\omega_k)\end{aligned}$$

where

$$\boldsymbol{T}_i(\omega_k) = \begin{bmatrix} 1 & 0 \\ \dfrac{-m_i\omega_k^2 + k_i}{\alpha_{i+1}^{ST}} & \dfrac{\alpha_i^{ST}}{\alpha_{i+1}^{ST}} \end{bmatrix}, \quad \boldsymbol{\delta T}_i(\omega_k) = \begin{bmatrix} 0 & 0 \\ \dfrac{2m_i\omega_k}{\alpha_{i+1}^{ST}} & 0 \end{bmatrix}$$

$$\boldsymbol{E}_i(\omega_k) = \begin{bmatrix} \dfrac{l_i}{c_i}S_{ik} & -\dfrac{l_i}{\omega_k}C_{ik} + \dfrac{c_i}{\omega_k^2}S_{ik} \\ \dfrac{\omega_k l_i}{c_i^2}C_{ik} + \dfrac{1}{c_i}S_{ik} & \dfrac{l_i}{c_i}S_{ik} \end{bmatrix} \tag{46}$$

with $S_{ik} = \sin(\omega_k l_i/c_i)$ and $C_{ik} = \cos(\omega_k l_i/c_i)$.

Because $\boldsymbol{Z}(\mathrm{j}\omega_k)$ is real, so is adj$\boldsymbol{Z}(\mathrm{j}\omega_k)$. Thus, the transfer function residues are given by

$$\boldsymbol{R}_k = -\mathrm{j}\boldsymbol{Q}_k, \quad \boldsymbol{R}_{-k} = \mathrm{j}\boldsymbol{Q}_k, \quad \mathrm{j} = \sqrt{-1} \tag{47}$$

where $\boldsymbol{Q}_k$ is a real matrix given by

$$\boldsymbol{Q}_k = \frac{\mathrm{adj}\,\boldsymbol{Z}(\mathrm{j}\omega_k)}{Z_D(\omega_k)} \tag{48}$$

5.3. Exact transient solution

According to matrix theory, adj$\boldsymbol{Z}(\mathrm{j}\omega_k)\boldsymbol{Z}(\mathrm{j}\omega_k) = \det\boldsymbol{Z}(\mathrm{j}\omega_k)\boldsymbol{I} = 0$. This implies that

$$\boldsymbol{R}_k\boldsymbol{Z}(\mathrm{j}\omega_k) = 0. \tag{49}$$

It follows from Eqs. (23), (40) and (49) that

$$\boldsymbol{R}_{\pm k}\boldsymbol{D}(x,\xi,\pm\mathrm{j}\omega_k) = \mp\mathrm{j}\boldsymbol{Q}_k\boldsymbol{M_b}\boldsymbol{U}^{-1}(\xi,\mathrm{j}\omega_k) \tag{50}$$

It is easy to see that $\boldsymbol{U}(x,\mathrm{j}\omega_k)$ and $\boldsymbol{U}(x,-\mathrm{j}\omega_k)$ are real and that $\boldsymbol{U}(x,\mathrm{j}\omega_k) = \boldsymbol{U}(x,-\mathrm{j}\omega_k)$. So Green's functions in Eq. (39) can be written as

$$\boldsymbol{G}(x,\xi,t) = 2\sum_{k=1}^{\infty}\boldsymbol{U}(x,\mathrm{j}\omega_k)\boldsymbol{Q}_k\boldsymbol{M_b}\boldsymbol{U}^{-1}(\xi,\mathrm{j}\omega_k)\sin\omega_k t$$

$$\boldsymbol{H}(x,t) = 2\sum_{k=1}^{\infty}\boldsymbol{U}(x,\mathrm{j}\omega_k)\boldsymbol{Q}_k\sin\omega_k t \tag{51}$$

Finally, by substituting Eq. (51) into Eq. (38), the transient response of the stepped system is obtained as follows:

$$\boldsymbol{\eta}(x,t) = 2\sum_{k=1}^{\infty}\boldsymbol{U}(x,\mathrm{j}\omega_k)\boldsymbol{Q}_k\{\boldsymbol{I}_{f,k}(t) + \boldsymbol{I}_{b,k}(t) + \boldsymbol{I}_{o,k}(t)\} \tag{52}$$

where

$$\boldsymbol{I}_{f,k}(t) = -\boldsymbol{M_b}\sum_{i=1}^{n}\frac{1}{\alpha_i^{ST}}\boldsymbol{U}^{-1}(x_{i-1}+,\mathrm{j}\omega_k)\int_0^t\int_{x_{i-1}}^{x_i}\mathrm{e}^{-\boldsymbol{F}_i(\mathrm{j}\omega_k)(\xi-x_{i-1})}\sin\omega_k(t-\tau)f_i(\xi,\tau)\,\mathrm{d}\xi\,\mathrm{d}\tau\begin{pmatrix}0\\1\end{pmatrix}$$

$$\boldsymbol{I}_{b,k}(t) = \int_0^t \sin\omega_k(t-\tau)\begin{pmatrix}\gamma_L(\tau)\\ \gamma_R(\tau)\end{pmatrix}\mathrm{d}\tau - \boldsymbol{M_b}\sum_{i=1}^{n-1}\frac{1}{\alpha_i^{ST}}\boldsymbol{U}^{-1}(x_i+,\mathrm{j}\omega_k)\int_0^t \sin\omega_k(t-\tau)(q_i(\tau)+k_iz_i(\tau))\,\mathrm{d}\tau\begin{pmatrix}0\\1\end{pmatrix} \tag{53}$$

$$\begin{aligned}\boldsymbol{I}_{o,k}(t) = {} & -\boldsymbol{M_b}\sum_{i=1}^{n}\frac{\rho_i}{\alpha_i^{ST}}\boldsymbol{U}^{-1}(x_{i-1}+,\mathrm{j}\omega_k)\int_{x_{i-1}}^{x_i}\mathrm{e}^{-\boldsymbol{F}_i(\mathrm{j}\omega_k)(\xi-x_{i-1})}(u_{0,i}(\xi)\omega_k\cos\omega_k t+v_{0,i}(\xi)\sin\omega_k t)\,\mathrm{d}\xi\begin{pmatrix}0\\1\end{pmatrix}\\ & -\boldsymbol{M_b}\sum_{i=1}^{n-1}\frac{m_i}{\alpha_{i+1}^{ST}}\boldsymbol{U}^{-1}(x_i+,\mathrm{j}\omega_k)(u_{0,i}(x_i)\omega_k\cos\omega_k t+v_{0,i}(x_i)\sin\omega_k t)\begin{pmatrix}0\\1\end{pmatrix}\\ & +\begin{pmatrix}m_Lu_{0,1}(x_0)\\ m_Ru_{0,n}(x_n)\end{pmatrix}\omega_k\cos\omega_k t+\begin{pmatrix}m_Lv_{0,1}(x_0)\\ m_Rv_{0,n}(x_n)\end{pmatrix}\sin\omega_k t\end{aligned}$$

The vectors $\boldsymbol{I}_{f,k}(t)$, $\boldsymbol{I}_{b,k}(t)$, and $\boldsymbol{I}_{o,k}(t)$ represent the contributions of external loads, boundary excitations and initial disturbances, respectively.

In summary of the above derivation, the remaining three terms takes the following three steps:

Step 1: Determine the natural frequencies of the stepped system by Eq. (32);

Step 2: Obtain the transfer function residues by Eqs. (47) and (48); and

Step 3: Compute the transient response by Eqs. (52) and (53).

The above transient solution is of exact form; no discretization or approximation has been made. This DTFM-based analysis is numerically efficient because it only involves operations of two-by-two matrices, regardless of the number of components. Furthermore, the method treats different system configurations (number of components, physical parameters, constraints, lumped masses, and boundary conditions) in a symbolic manner, and avoids tedious derivations and messy expressions that are encountered in many analytical methods.

6. Examples

The DTFM-based transient analysis is demonstrated in two examples: a single-body elastic bar in longitudinal vibration and a three-segment shaft in torsional vibration.

6.1. Example 1: An elastic bar in longitudinal vibration

In this example, we show that exact transient solutions obtained by the DTFM are equivalent to those by standard eigenfunction expansion. Consider a clamped-free single-body elastic bar whose longitudinal vibration is governed by

$$\text{Governing equation}: \quad \rho\frac{\partial^2 u(x,t)}{\partial t^2} - EA\frac{\partial^2 u(x,t)}{\partial x^2} = q(x,t), \quad x\in(0,L) \tag{54a}$$

$$\text{Boundary conditions}: \quad u(0,t)=0, \quad EA\frac{\partial u(L,t)}{\partial x} = p_b(t) \tag{54b}$$

$$\text{Initial conditions}: \quad u(x,0)=u_0(x), \quad \frac{\partial u(x,0)}{\partial t} = v_0(x), \quad x\in(0,L) \tag{54c}$$

where $q(x,t)$ is an external force applied at the interior points of the bar, $p_b(t)$ is a boundary load, and $u_0(x)$, $v_0(x)$ are the initial displacement and velocity of the bar.

First obtain the transient response of the bar by eigenfunction expansion. The displacement of the bar is expressed as [21]

$$u(x,t) = \int_0^t\int_0^t g(x,\xi,t-\tau)q(\xi,\tau)\,\mathrm{d}\xi\,\mathrm{d}\tau + \int_0^L\left[\frac{\partial}{\partial t}g(x,\xi,t)\rho u_0(\xi)+g(x,\xi,t)\rho v_0(\xi)\right]\mathrm{d}\xi + \int_0^t g(x,L,t-\tau)p_b(\tau)\,\mathrm{d}\tau \tag{55}$$

where $g(x,\xi,t)$ is Green's function of the bar, and it is obtained in an eigenfunction series:

$$g(x,\xi,t) = \sum_{k=1}^{\infty}\frac{1}{\omega_k}v_k(x)v_k(\xi)\sin\omega_k t \tag{56}$$

with ω_k and $v_k(x)$ being the kth natural frequency and normalized eigenfunction of the bar. The system eigensolutions are found as

$$\omega_k = \left(k-\frac{1}{2}\right)\pi\frac{c}{L}, \quad v_k(x) = \sqrt{\frac{2}{\rho L}}\sin\left(\frac{\omega_k x}{c}\right) \tag{57}$$

with $c=\sqrt{EA/\rho}$. Substituting Eqs. (56) and (57) into Eq. (55) to get the transient response

$$u(x,t)=\frac{2}{\rho L}\sum_{k=1}^{\infty}\frac{1}{\omega_k}\sin\frac{\omega_k x}{c}\left\{\int_0^t\int_0^L \sin\frac{\omega_k\xi}{c}\sin\omega_k(t-\tau)q(\xi,\tau)\,\mathrm{d}\xi\,\mathrm{d}\tau+\int_0^L\sin\left(\frac{\omega_k}{c}\xi\right)(\rho u_0(\xi)\omega_k\cos\omega_k t\right.$$
$$\left.+\rho v_0(\xi)\sin\omega_k t)\,\mathrm{d}\xi+(-1)^{k+1}\int_0^L\sin\omega_k(t-\tau)p_b(\tau)\,\mathrm{d}\tau\right\} \tag{58}$$

Next determine the bar response by the DTFM. The matrices in Eqs. (11), (13) and (14) are

$$\boldsymbol{F}(s)=\begin{bmatrix}0 & 1\\ \rho s^2/EA & 0\end{bmatrix},\quad \boldsymbol{M_b}=\begin{bmatrix}1 & 0\\ 0 & 0\end{bmatrix},\quad \boldsymbol{N_b}=\begin{bmatrix}0 & 0\\ 0 & EA\end{bmatrix} \tag{59}$$

The boundary impedance matrix in Eq. (26) is

$$\boldsymbol{Z}(s)=\begin{bmatrix}1 & 0\\ \dfrac{EAs}{c}\sinh\left(\dfrac{sL}{c}\right) & EA\cosh\left(\dfrac{sL}{c}\right)\end{bmatrix} \tag{60}$$

The characteristic equation then is

$$\det\boldsymbol{Z}(s)=EA\cosh\left(\frac{sL}{c}\right)=0 \tag{61}$$

which has the roots $s_k=\mathrm{j}\omega_k$, with $\mathrm{j}=\sqrt{-1}$ and ω_k being the same as in Eq. (57). By Eq. (47), the transfer function residues are obtained as

$$\boldsymbol{R}_k=-\mathrm{j}\begin{bmatrix}0 & 0\\ \dfrac{\omega_k}{L} & \dfrac{(-1)^{k+1}c}{EAL}\end{bmatrix},\quad k=1,2,\ldots \tag{62}$$

With Eqs. (52) and (53), the displacement of the bar is given by

$$u(x,t)=\frac{2c^2}{EAL}\sum_{k=1}^{\infty}\frac{1}{\omega_k}\sin\frac{\omega_k x}{c}\boldsymbol{E}_k\{\boldsymbol{I}_{f,k}(t)+\boldsymbol{I}_{b,k}(t)+\boldsymbol{I}_{o,k}(t)\} \tag{63}$$

where

$$\boldsymbol{E}_k=\begin{bmatrix}\dfrac{EA\omega_k}{c} & (-1)^{k+1}\end{bmatrix}$$

$$\boldsymbol{I}_{f,k}(t)=-\frac{1}{EA}\boldsymbol{M_b}\int_0^t\int_0^L \mathrm{e}^{-\boldsymbol{F}(\mathrm{j}\omega_k)\xi}\sin\omega_k(t-\tau)q(\xi,\tau)\,\mathrm{d}\xi\,\mathrm{d}\tau\begin{pmatrix}0\\1\end{pmatrix}$$

$$\boldsymbol{I}_{b,k}(t)=\int_0^t\sin\omega_k(t-\tau)p_b(\tau)\,\mathrm{d}\tau\begin{pmatrix}0\\1\end{pmatrix}$$

$$\boldsymbol{I}_{o,k}(t)=-\frac{1}{EA}\boldsymbol{M_b}\int_0^L \mathrm{e}^{-\boldsymbol{F}(\mathrm{j}\omega_k)\xi}\{\rho u_0(\xi)\omega_k\cos\omega_k t+\rho v_0(\xi)\sin\omega_k t\}\,\mathrm{d}\xi\begin{pmatrix}0\\1\end{pmatrix} \tag{64}$$

From Eqs. (34) and (59), it is easy to show that

$$\boldsymbol{E}_k\begin{pmatrix}0\\1\end{pmatrix}=(-1)^{k+1},\quad \boldsymbol{E}_k\boldsymbol{M_b}=\begin{pmatrix}\dfrac{EA\omega_k}{c} & 0\end{pmatrix},\quad \mathrm{e}^{-F(\mathrm{j}\omega_k)\xi}\begin{pmatrix}0\\1\end{pmatrix}=\begin{pmatrix}-\dfrac{c}{\omega_k}\sin\dfrac{\omega_k\xi}{c}\\ \cos\dfrac{\omega_k\xi}{c}\end{pmatrix}$$

As a result

$$\boldsymbol{E}_k\boldsymbol{I}_{f,k}(t)=\int_0^t\int_0^L\sin\frac{\omega_k\xi}{c}\sin\omega_k(t-\tau)q(\xi,\tau)\,\mathrm{d}\xi\,\mathrm{d}\tau$$

$$\boldsymbol{E}_k\boldsymbol{I}_{b,k}(t)=(-1)^{k+1}\int_0^t\sin\omega_k(t-\tau)p_b(\tau)\,\mathrm{d}\tau$$

$$\boldsymbol{E}_k\boldsymbol{I}_{o,k}(t)=\int_0^L\sin\frac{\omega_k\xi}{c}\{\rho u_0(\xi)\omega_k\cos\omega_k t+\rho v_0(\xi)\sin\omega_k t\}\,\mathrm{d}\xi$$

Substitution of the previous equations into Eq. (63) and use of $c^2=EA/\rho$ yield the same result as given in Eq. (58), although no eigenfunctions have been used in this DTFM-based analysis.

It should be pointed out that the expressions of $\boldsymbol{Z}(s)$ and $\boldsymbol{R}_k$ are shown in Eqs. (60) and (62) for demonstrative purposes. The derivation of these analytical expressions is not needed in the DTFM-based computation.

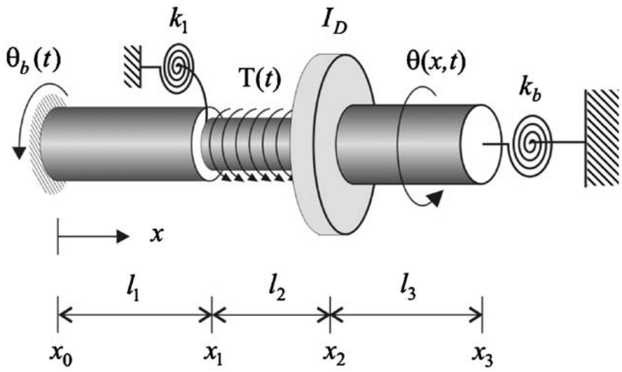

Fig. 2. A three-segment circular shaft in torsional vibration.

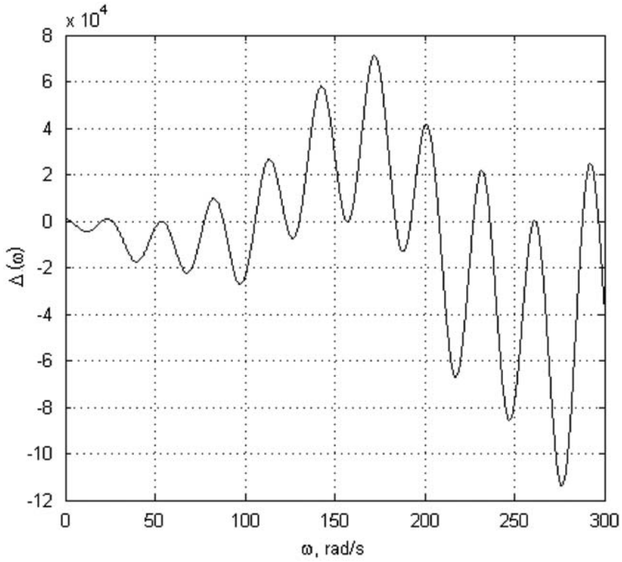

Fig. 3. Characteristic function of the stepped shaft.

6.2. Example 2: A three-segment shaft in torsional vibration

In Fig. 2a three-segment circular shaft in torsional vibration is fixed at the left end, is constrained by two springs (k_1 and k_b), and carries a rigid disk with mass moment of inertia I_D. For numerical simulation, the physical parameters of the system are assigned as follows:

$$\begin{aligned} &\text{Segment 1}: \quad \rho_v J_1 = 2.0\,\text{kg m}, \quad GJ_1 = 400\,\text{N m}^2, \quad l_1 = 1.0\,\text{m} \\ &\text{Segment 2}: \quad \rho_v J_2 = 1.5\,\text{kg m}, \quad GJ_2 = 300\,\text{N m}^2, \quad l_2 = 0.7\,\text{m} \\ &\text{Segment 3}: \quad \rho_v J_3 = 1.2\,\text{kg m}, \quad GJ_3 = 250\,\text{N m}^2, \quad l_3 = 1.3\,\text{m} \\ &k_1 = 50\,\text{N m}, \quad k_b = 100\,\text{N m}, \quad I_D = 25\,\text{kg m}^2 \end{aligned} \tag{65}$$

The natural frequencies of the shaft are determined through the solution of Eq. (32) by the bisection method. The transcendental characteristic function $\Delta(\omega)$ is plotted against ω in Fig. 3. Table 2 gives the first 20 natural frequencies and several higher-mode frequencies of the shaft, which are computed by the proposed DTFM and a finite element method (FEM) that uses linear shape functions. As the number of elements increases, the FEM solutions converge to the exact solutions provided by the DTFM. The FEM with 150 and 300 elements gives good results on the first 20 natural frequencies, with maximum errors of 0.69% and 0.17%, respectively. However, errors in the FEM predictions grow when higher-mode natural frequencies are computed. With 300 elements, the FEM has a 4.43% error in estimating the 100th natural frequency, and a 16.72% error in estimating the 200th natural frequency. As found out in a further comparison, to match the accuracy of the DTFM solutions (with the maximum error less than 0.4%), 1200 finite elements are needed to predict the first 100 natural frequencies and at least 2000 finite elements are needed to estimate the first 200 natural frequencies. The enlarged number of elements translates into significant demand for computation time by the FEM.

Table 2
The natural frequencies ω_k of the stepped shaft (in rad/s).

k	DTFM	Finite element method		
		30 elements	150 elements	300 elements
1	3.25798	3.25799	3.25798	3.25798
2	20.80147	20.81898	20.80217	20.80165
3	26.33416	26.37154	26.33565	26.33453
4	53.47210	53.78622	53.48464	53.47523
5	53.76396	54.07707	53.77646	53.76709
6	77.40565	78.37285	77.44421	77.41529
7	88.01690	89.38396	88.07135	88.03051
8	105.66194	108.13073	105.76016	105.68649
9	122.66715	126.38157	122.81472	122.70403
10	130.30087	134.93928	130.48513	130.34692
11	156.73334	164.81820	157.05419	156.81351
12	157.42196	165.29005	157.73408	157.49995
13	183.81502	196.84198	184.33276	183.94438
14	192.21769	206.52036	192.78611	192.35970
15	208.02260	226.82940	208.77331	208.21013
16	227.04101	250.41870	227.97814	227.27508
17	236.42430	263.72538	237.52678	236.69964
18	260.56758	296.46058	262.04388	260.93621
19	261.88047	297.02135	263.31926	262.23974
20	287.77085	334.51074	289.76037	288.26751
25	366.44324	440.38406	370.39112	367.42808
30	436.17403	497.67631	442.83877	437.83536
50	732.01238		764.96904	740.20894
100	1482.48060		1726.74748	1548.17924
200	2979.78780			3478.02958

Although system eigenfunctions are not required in the DTFM-based transient analysis, they are often examined for free vibration analysis and for understanding of system dynamic characteristics. By Eq. (37), the first five mode shapes and the 17th mode shape of the stepped shaft are plotted in Fig. 4, where a kink at the disk location ($x_2 = 1.7$ m) is seen in some mode shapes. The 17th mode shape shall be used for comparison with the shaft response subject to a boundary excitation.

In what follows, we consider two cases of transient response: response to an external torque, and response to a boundary excitation. A precursor convergence study shows that the transient responses computed with 100 terms or more from the series (52) are not much different from those obtained with 50 terms. For this reason, only the first 50 terms in the series are used to present the transient solutions.

Response to external torque: Consider a toque $T(t)$ that is uniformly applied to the second shaft segment (see Fig. 2)

$$f_2(x,t) = T_0(1 - \mathrm{e}^{-\sigma t}), \quad x \in (x_1, x_2) \tag{66}$$

where T_0 and σ are positive constants. Assume zero initial disturbances. The transient response of the shaft, by Eqs. (52) and (53), is

$$\boldsymbol{\eta}(x,t) = \frac{2}{GJ_2}\sum_{k=1}^{\infty} q_k(t)\boldsymbol{U}(x,\mathrm{j}\omega_k)\boldsymbol{Q}_k\boldsymbol{M_b}\boldsymbol{U}^{-1}(x_1+,\mathrm{j}\omega_k)\begin{pmatrix}\lambda_k^2[1-\cos(l_2/\lambda_k)]\\ -\lambda_k\sin(l_2/\lambda_k)\end{pmatrix} \tag{67}$$

where $\lambda_k = c_2/\omega_k$, and

$$q_k(t) = T_0\left\{\frac{1}{\omega_k}(1-\cos\omega_k t) + \frac{1}{\omega_k^2+\sigma^2}(\omega_k\cos\omega_k t - \sigma\sin\omega_k t - \omega_k \mathrm{e}^{-\sigma t})\right\} \tag{68}$$

Select $T_0 = 2.5$ N and $\sigma = 10\,\mathrm{s}^{-1}$. The rotation θ and shear strain $\partial\theta/\partial x$ of the stepped shaft at times t=0, 0.1, 0.3, 0.5, 0.7 and 1 s are plotted in Fig. 5. Note that the shear strain profile in Fig. 5b has jumps, which are caused by nonuniform distribution of geometric and material properties, the spring constraint at node x_1, and the rigid disk at node x_2.

It is worthy of pointing out that conventional series solution methods, such as Galerkin method and Rayleigh–Ritz method, are inefficient in portraying the discontinuities in strain as seen in Fig. 5b. These methods represent the solution by a sequence of functions whose spatial derivatives are continuous over the entire domain. As such, many terms are required to describe the abrupt changes in $\partial\theta/\partial x$ and the results still may not be satisfactory due to issues like Gibbs phenomenon. The proposed DTFM automatically produces piecewise-continuous spatial derivatives in the solution, which is facilitated by matrices $\boldsymbol{T}_i$ in the matching conditions (13). And this is done without the need for a large number of terms.

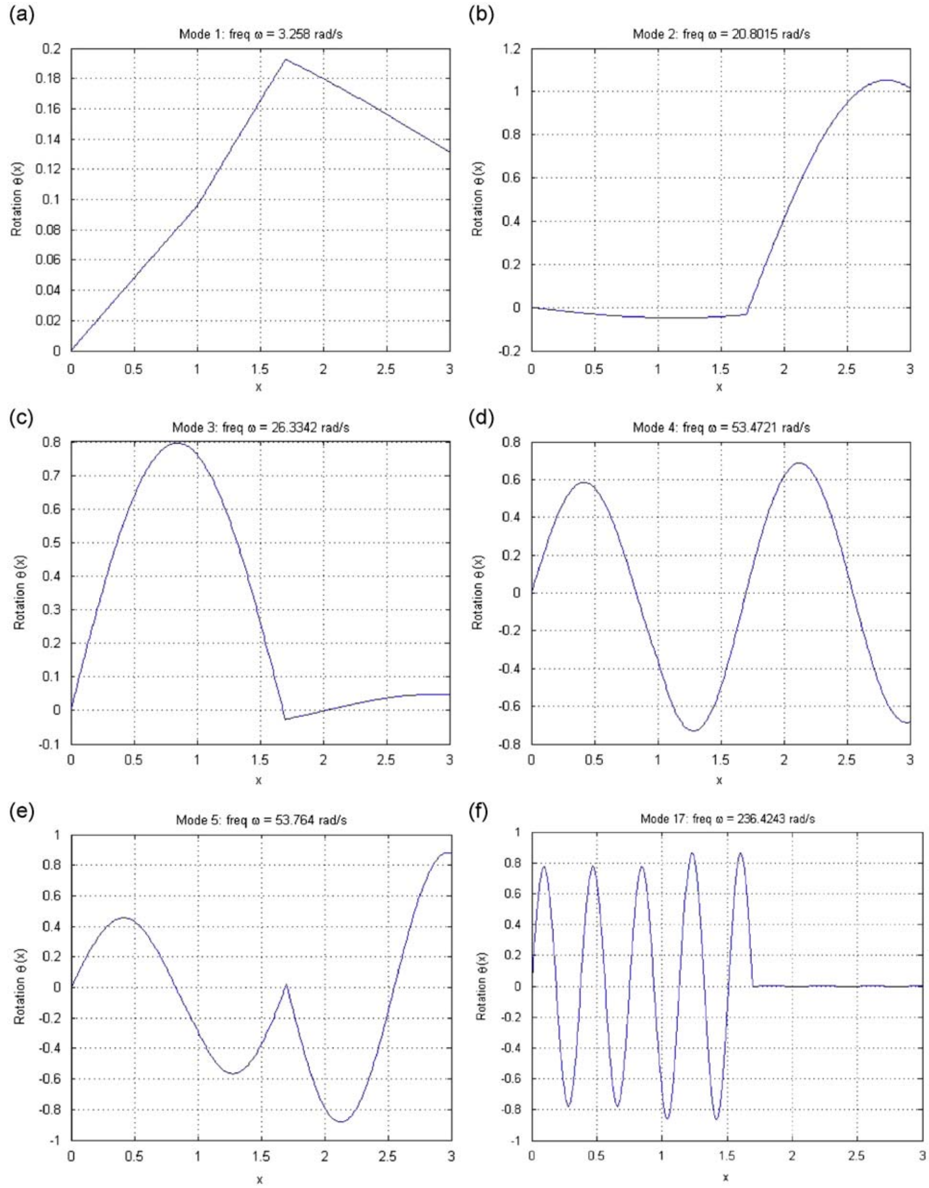

Fig. 4. Mode shapes of the stepped shaft: (a) mode 1; (b) mode 2; (c) mode 3; (d) mode 4; (e) mode 5; and (f) mode 17.

In fact, 10 terms are good enough to present the spatial discontinuities of the current problem; see Fig. 6 where $\partial\theta/\partial x$ at $t=1$ s is plotted by using 10, 20 and 50 terms from Eq. (67).

Response to boundary excitation: The shaft is subject to a sinusoidal boundary displacement at its left end (see Fig. 2)

$$\theta_1(0,t)=\theta_b(t)=\Theta_0\sin\omega t \tag{69}$$

The transient response of the stepped system is

$$\boldsymbol{\eta}(x,t)=2\sum_{k=1}^{\infty}q_k(t)\boldsymbol{U}(x,\mathrm{j}\omega_k)\mathbf{Q}_k\begin{pmatrix}1\\0\end{pmatrix} \tag{70}$$

where

$$q_k(t)=\begin{cases}\dfrac{\Theta_0}{\omega_k^2-\omega^2}(\omega_k\sin\omega t-\omega\sin\omega_k t), & \text{for } \omega\neq\omega_k\\ \dfrac{\Theta_0}{2\omega_k}(\sin\omega_k t-\omega_k t\cos\omega_k t), & \text{for } \omega=\omega_k\end{cases} \tag{71}$$

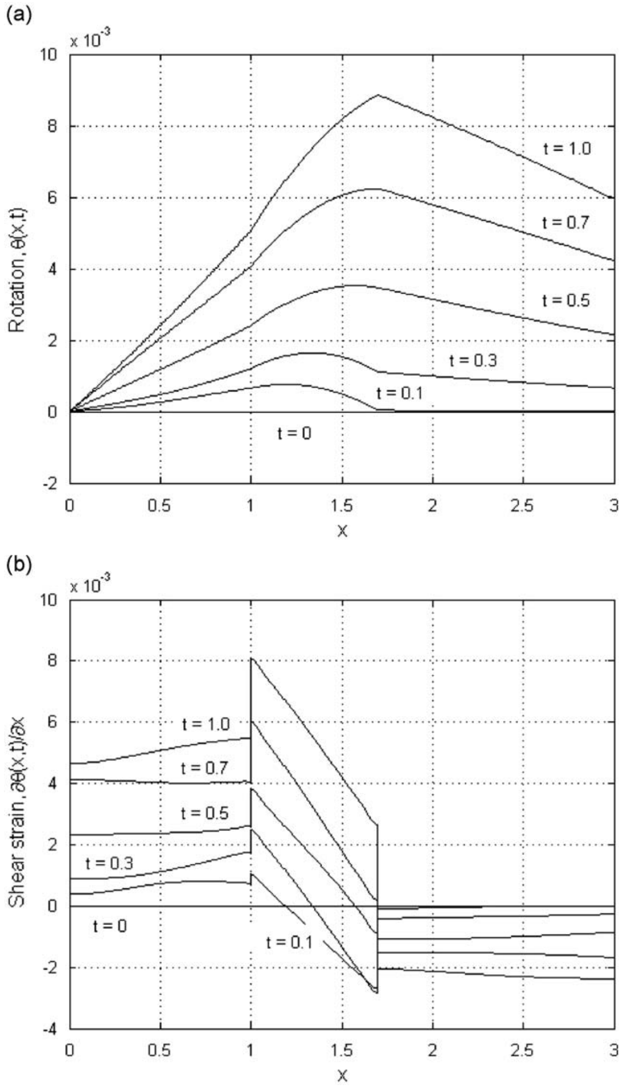

Fig. 5. Transient response of the stepped shaft subject to the uniform torque given by Eq. (65): (a) rotation distributions in rad; (b) shear strain distributions in rad/m.

Choose $\Theta_0 = 0.005$ rad and $\omega = 236$ rad/s. By Eqs. (70) and (71), the rotation profiles of the shaft at times t=0.05, 0.1, 0.15, 0.2 and 4 s are plotted in Fig. 7. The vibration of the shaft at early times can be viewed as waves traveling rightward on the shaft, as shown in Figs. 7(a) and (b). The time for the boundary disturbances to reach the rigid disk (at $x_2 = 1.7$ m) can be approximately estimated as

$$l_1/\sqrt{GJ_1/\rho_v J_1} + l_2/\sqrt{GJ_2/\rho_v J_2} = 0.1202\,\text{s} \tag{72}$$

Shortly after the initial disturbances arrive at the disk location (x=1.7 m), some of the waves are transmitted to the third segment and continue traveling rightward; others are reflected back to the second segment and move leftward. This is seen in Figs. 7(c) and (d). Before soon, the vibration of the shaft becomes a mixture of incoming waves (disturbances from x=0), transmitted waves and reflected waves; for instance see Fig. 7(e). After a long enough time, the vibration settles in a specific pattern; see Fig. 7(f), where the vibration amplitude of the first and second shaft segments is significantly larger than that of the third segment. This is because the excitation frequency is near the 17th natural frequency of the shaft, ω_{17}=236.4243 rad/s. For comparison, see the 17th mode shape in Fig. 4(f). Therefore, the pattern in Fig. 7(f) is a reflection of dominancy of the 17th mode shape in the shaft vibration.

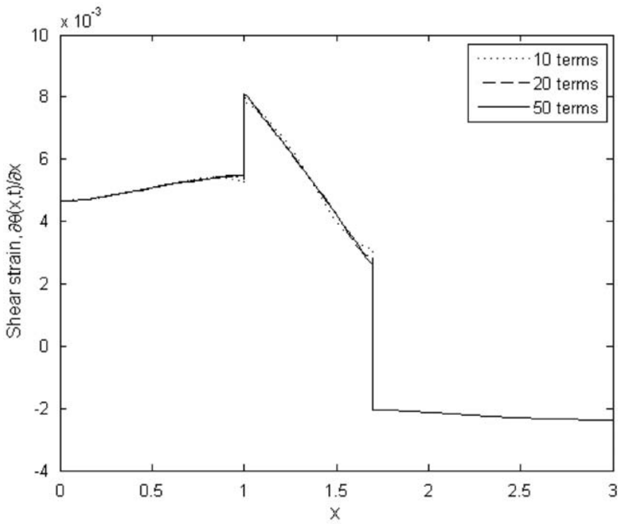

Fig. 6. Distribution of shear strain $\partial\theta/\partial x$ (in rad/m) of the shaft subject to the uniform torque at time t=1 s, computed with first 10, 20 and 50 terms from series (67).

7. Conclusions

The distributed transfer function method developed for transient analysis of stepped distributed systems has the following features.

(a) The DTFM is the first Laplace-transform-based analytical method that delivers exact transient solutions for stepped systems of any number of distributed components and lumped masses, and subject to combined external, boundary and initial disturbances. The highlight of the method is that it in transient analysis gives exact transfer function residues, without having to deal with tedious derivations and possible errors caused by singularities of system transfer functions.

(b) The DTFM describes stepped distributed systems with a compact spatial state formulation. Nonuniform distribution of physical parameters and general boundary conditions are systematically treated through easy assignment of state matrices $\boldsymbol{F}_j$, boundary matrices $\boldsymbol{M_b}$ and $\boldsymbol{N_b}$, and constraint matrices $\boldsymbol{T}_i$. The solution procedure is the same for different system configurations and various excitations. Furthermore, the DTFM-based computation only requests simple operations of two-by-two matrices. The symbolic feature and low-order matrix manipulation make the DTFM highly efficient in numerical simulation, as has been shown in Section 6.

(c) The DTFM is different from existing series solution methods in two major aspects. First, unlike eigenfunction expansion technique, the DTFM in transient analysis does not use system eigenfunctions, and in computation does not need to deal with spatial integrals for normalization of system eigenfunctions. Second, many series solution methods require different derivations for different system configurations (number of components, boundary conditions, constraints and lumped masses, etc.). The DTFM adopts a symbolic formulation, Eqs. (9), (13) and (14), which systematically treats different configurations by formula (52). This symbolic manipulation feature renders the DTFM user-friendly.

(d) Facilitated by matrices $\boldsymbol{T}_i$ in the fundamental matrix of Eq. (21), the DTFM is capable of producing piecewise-continuous spatial derivatives in a solution, as demonstrated in Fig. 5. Piecewise-continuous spatial derivatives are required to portrait jumps in stress or strain for continua with nonuniform geometric and material properties. Conventional series methods, such as Rayleigh–Ritz method and Galerkin method, do not have this capability as they employ a sequence of functions whose spatial derivatives are continuous in the entire domain. This feature makes the DTFM quite useful for dynamic analysis of continua with geometric and material discontinuities.

While only uniform distributed components are considered in this work, the proposed transient analysis can be generalized to include certain nonuniform components whose inertia and stiffness parameters are functions of spatial coordinate x. For instance, exact transient solutions of shafts and bars with tapered, conical, and exponential cross sections may be obtained by the DTFM. One key in this generalization is to replace exponential matrices $e^{F_i(s)x}$ by appropriate state transition matrices for the related nonuniform components. An investigation on this subject is underway.

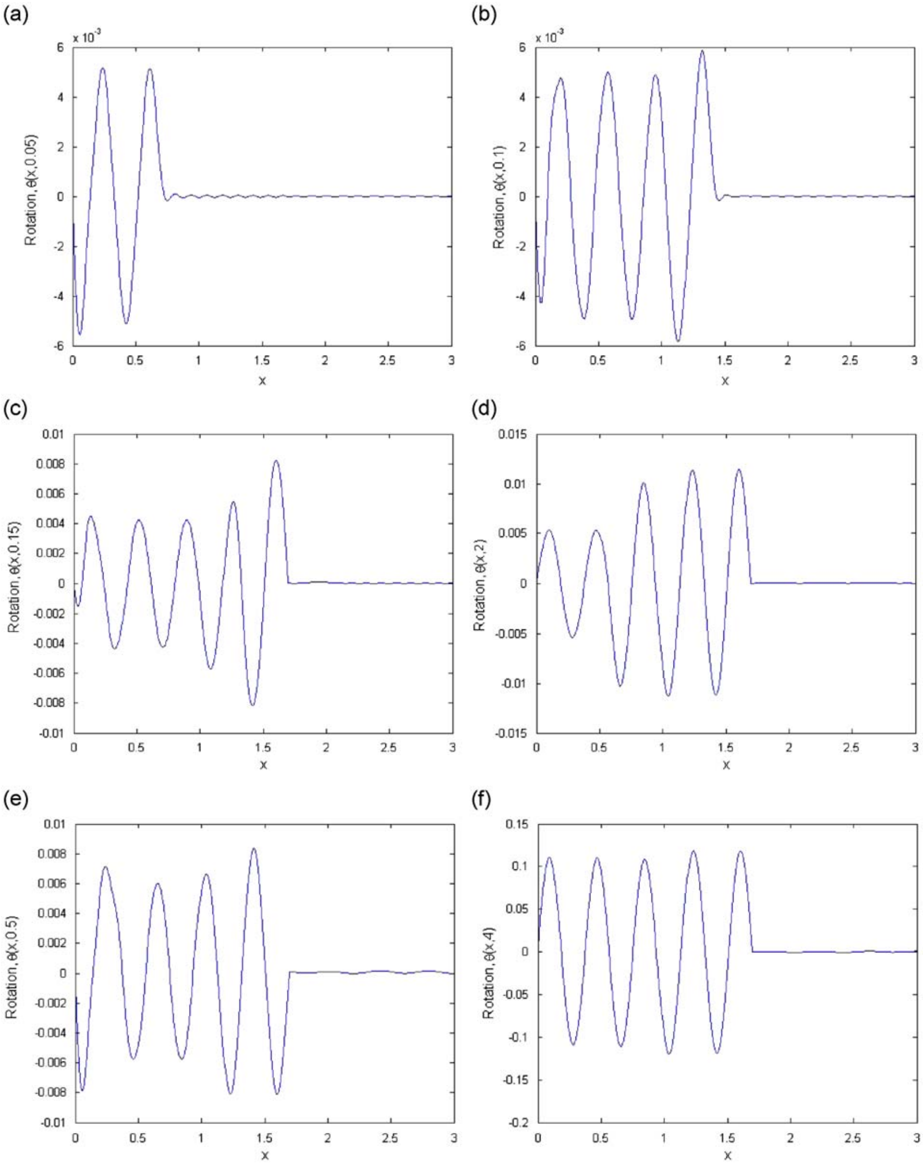

Fig. 7. Transient displacement profiles of the shaft subject to the sinusoidal boundary excitation $\theta_b(t) = \Theta_0 \sin \omega t$, with $\Theta_0 = 0.05$ rad, ω=236 rad/s: (a) t=0.05 s; (b) t=0.1 s; (c) t=0.15 s; (d) t=0.2 s; (e) t=0.5 s; and (f) t=4 s.

Acknowledgments

This work was a result of the author's previous projects partially sponsored by the US Army Research Office and NASA's Jet Propulsion Laboratory.

Appendix A. Proof of Eq. (24)

By Eqs. (24) and (25)

$$\hat{\boldsymbol{\eta}}(x,s) = \boldsymbol{\Phi}(x,x_0,s)\boldsymbol{Z}^{-1}(s)\left\{\boldsymbol{M_b}\int_{x_0}^{x}\boldsymbol{\Phi}(x_0,\xi,s)\hat{\boldsymbol{p}}(\xi,s)\,\mathrm{d}\xi - \boldsymbol{N_b}\int_{x}^{x_n}\boldsymbol{\Phi}(x_n,\xi,s)\hat{\boldsymbol{p}}(\xi,s)\,\mathrm{d}\xi + \boldsymbol{\gamma_b}(s)\right\} - \boldsymbol{\Phi}(x,x_0,s)\boldsymbol{Z}^{-1}(s)\sum_{i=1}^{n-1}\boldsymbol{D}(x,x_i+,s)\mathbf{v}_i(s) \tag{A.1}$$

where

$$D(x,x_i+,s)=\begin{cases}\boldsymbol{M_b}\boldsymbol{\Phi}(x_0,x_i+,s) & \text{for } x_i+\le x\\ -\boldsymbol{N_b}\boldsymbol{\Phi}(x_n,x_i+,s) & \text{for } x_i+>x\end{cases} \tag{A.2}$$

Differentiate the both sides of Eq. (A.1) and use the properties (18), to obtain

$$\begin{aligned}\frac{\partial}{\partial x}\hat{\boldsymbol{\eta}}(x,s)&=\boldsymbol{F}(x,s)\hat{\boldsymbol{\eta}}(x,s)+\boldsymbol{\Phi}(x,x_0,s)\boldsymbol{Z}^{-1}(s)(\boldsymbol{M_b}\boldsymbol{\Phi}(x_0,x,s)+\boldsymbol{N_b}\boldsymbol{\Phi}(x_n,x,s))\hat{\boldsymbol{p}}(x,s)\\&=\boldsymbol{F}(x,s)\hat{\boldsymbol{\eta}}(x,s)+\boldsymbol{\Phi}(x,x_0,s)\boldsymbol{Z}^{-1}(s)\boldsymbol{Z}(s)\boldsymbol{\Phi}(x_0,x,s)\hat{\boldsymbol{p}}(x,s)=\boldsymbol{F}(x,s)\hat{\boldsymbol{\eta}}(x,s)+\hat{\boldsymbol{p}}(x,s)\end{aligned}$$

This means that Eq. (A.1) satisfies the state Eq. (11). Now, use Eq. (A.1) to compute

$$\begin{aligned}\boldsymbol{M_b}\hat{\boldsymbol{\eta}}(x_0,s)+\boldsymbol{N_b}\hat{\boldsymbol{\eta}}(x_n,s)&=\boldsymbol{M_b}\boldsymbol{Z}^{-1}(s)\left(\gamma_b(s)-\boldsymbol{N_b}\boldsymbol{\Phi}(x_n,x_0,s)\int_{x_0}^{x_n}\boldsymbol{\Phi}(x_0,\xi,s)\hat{\boldsymbol{p}}(\xi,s)\,\mathrm{d}\xi\right)\\&\quad+\boldsymbol{N_b}\boldsymbol{\Phi}(x_n,x_0,s)\boldsymbol{Z}^{-1}(s)\left(\gamma_b(s)+\boldsymbol{M_b}\int_{x_0}^{x_n}\boldsymbol{\Phi}(x_0,\xi,s)\hat{\boldsymbol{p}}(\xi,s)\,\mathrm{d}\xi\right)\\&\quad+\sum_{i=1}^{n-1}\{\boldsymbol{M_b}\boldsymbol{\Phi}(x_0,x_0,s)\boldsymbol{Z}^{-1}(s)\boldsymbol{N_b}\boldsymbol{\Phi}(x_n,x_i+,s)-\boldsymbol{N_b}\boldsymbol{\Phi}(x_n,x_0,s)\\&\quad\times\boldsymbol{Z}^{-1}(s)\boldsymbol{M_b}\boldsymbol{\Phi}(x_0,x_i+,s)\mathbf{v}_i(s)\}\\&=\boldsymbol{M_b}\boldsymbol{Z}^{-1}(s)\left(\boldsymbol{\gamma_b}(s)+(\boldsymbol{M_b}-\boldsymbol{Z}(s))\int_{x_0}^{x_n}\boldsymbol{\Phi}(x_0,\xi,s)\hat{\boldsymbol{p}}(\xi,s)\,\mathrm{d}\xi\right)\\&\quad+(\boldsymbol{Z}(s)-\boldsymbol{M_b})\boldsymbol{Z}^{-1}(s)\times\left(\boldsymbol{\gamma_b}(s)+\boldsymbol{M_b}\int_{x_0}^{x_n}\boldsymbol{\Phi}(x_0,\xi,s)\hat{\boldsymbol{p}}(\xi,s)\,\mathrm{d}\xi\right)\\&\quad+\sum_{i=1}^{n-1}\{\boldsymbol{M_b}\boldsymbol{Z}^{-1}(s)(\boldsymbol{Z}(s)-\boldsymbol{M_b}-(\boldsymbol{Z}(s)-\boldsymbol{M_b})\boldsymbol{Z}^{-1}(s)\boldsymbol{M_b}\}\boldsymbol{\Phi}(x_0,x_i+,s)\mathbf{v}_i(s)\\&=\boldsymbol{\gamma_b}(s)\end{aligned}$$

where $\boldsymbol{N_b}\boldsymbol{\Phi}(x_n,x_0,s)=\boldsymbol{Z}(s)-\boldsymbol{M_b}$ and Eq. (18) have been used. So, Eq. (A.1) satisfies the boundary condition (14). Finally, by Eqs. (A.1), (A.2) and (17),

$$\begin{aligned}\hat{\boldsymbol{\eta}}(x_j+,s)&=\boldsymbol{T}_j\boldsymbol{\Phi}(x_j-,x_0,s)\boldsymbol{Z}^{-1}(s)\{\boldsymbol{M_b}\int_{x_0}^{x_j-}\boldsymbol{\Phi}(x_0,\xi,s)\hat{\boldsymbol{p}}(\xi,s)\,\mathrm{d}\xi-\boldsymbol{N_b}\int_{x_j-}^{x_n}\boldsymbol{\Phi}(x_n,\xi,s)\hat{\boldsymbol{p}}(\xi,s)\,\mathrm{d}\xi\\&\quad+\boldsymbol{\gamma_b}(s)\}-\boldsymbol{T}_j\boldsymbol{\Phi}(x_j-,x_0,s)\boldsymbol{Z}^{-1}(s)\sum_{i=1}^{n-1}\boldsymbol{D}(x_j-,x_i+,s)\mathbf{v}_i(s)\\&\quad-\boldsymbol{T}_j\boldsymbol{\Phi}(x_j-,x_0,s)\boldsymbol{Z}^{-1}(s)\boldsymbol{Z}(s)\boldsymbol{\Phi}(x_0,x_j-,s)\boldsymbol{T}_j^{-1}\mathbf{v}_i(s)=\boldsymbol{T}_j\hat{\boldsymbol{\eta}}(x_j-,s)-\mathbf{v}_i(s)\end{aligned}$$

This shows that Eq. (A.1) also satisfies the matching condition (13). Therefore, Eqs. (24) and (25) provide the unique solution of Eq. (11) subject to conditions (13) and (14).

Appendix B. Proof of Eq. (43)

It is easy to show that

$$\frac{\mathrm{d}}{\mathrm{d}s}|\boldsymbol{Z}(s)|=\det\left(\boldsymbol{M_b}+\boldsymbol{N_b}\frac{\mathrm{d}\boldsymbol{U}(x_n,s)}{\mathrm{d}s}\right)+\det\left(\frac{\mathrm{d}\boldsymbol{M_b}}{\mathrm{d}s}+\boldsymbol{N_b}\boldsymbol{U}(x_n,s)\right)+\det\left(\boldsymbol{M_b}+\frac{\mathrm{d}\boldsymbol{N_b}}{\mathrm{d}s}\boldsymbol{U}(x_n,s)\right) \tag{B.1}$$

By Eq. (21)

$$\frac{\mathrm{d}\boldsymbol{U}(x_n,s)}{\mathrm{d}s}=\frac{\mathrm{d}}{\mathrm{d}s}(\mathrm{e}^{\boldsymbol{F}_n(s)l_n}\boldsymbol{T}_{n-1}\mathrm{e}^{\boldsymbol{F}_{n-1}(s)l_{n-1}}\cdots\boldsymbol{T}_1\mathrm{e}^{\boldsymbol{F}_1(s)l_1}) \tag{B.2}$$

and with Eq. (22)

$$\frac{\mathrm{d}}{\mathrm{d}s}(\mathrm{e}^{\boldsymbol{F}_i(s)l_i})_{s=\mathrm{j}\omega_k}=\mathrm{j}\boldsymbol{E}_i(\omega_k) \tag{B.3}$$

where $\boldsymbol{E}_i(\omega_k)$ is given in Eq. (46). Note that $\mathrm{e}^{\boldsymbol{F}_i(\mathrm{j}\omega_k)l_i}$, $\boldsymbol{M_b}|_{s=\mathrm{j}\omega_k}$ and $\boldsymbol{N_b}|_{s=\mathrm{j}\omega_k}$ all are real matrices. Substituting Eqs. (B.2) to (B.3) into Eq. (B.1) yields Eq. (43).

References

[1] J.C. Snowdon, *Vibration and Shock in Damped Mechanical Systems*, Wiley, New York, 1968.
[2] D.J. Gorman, *Free Vibration Analysis of Beams and Shafts*, Wiley, New York, 1975.
[3] A.D. Dimarogonas, S.A. Paipeties, *Analytical Methods in Rotor Dynamics*, Applied Science Publishers, New York, 1983.
[4] M.L. Munjal, A.V. Sreenath, M.V. Narasimhan, An algebraic algorithm for the design and analysis of linear dynamical systems, *Journal of Sound and Vibration* 26 (1973) 193–208.

[5] A. Mioduchowski, Torsional waves and free vibrations of drive systems with stepped shafts, *Ingenieur Archiv* 56 (1986) 314–320.
[6] C.N. Bapat, N. Bhutani, General approach for free and forced vibrations of stepped systems governed by the one-dimensional wave equation with non-classical boundary conditions, *Journal of Sound and Vibration* 172 (1994) 1–22.
[7] B. Yang, Linear vibration of a coupled string-rigid bar system, *Journal of Sound and Vibration* 183 (1995) 383–399.
[8] W.-J. Hsueh, Free and forced vibrations of stepped rods and coupled systems, *Journal of Sound and Vibration* 226 (1999) 891–904.
[9] Q.S. Li, Torsional vibration of multi-step non-uniform rods with various concentrated elements, *Journal of Sound and Vibration* 260 (2003) 637–651.
[10] B. Yang, Closed-form transient response of distributed damped systems, part ii: energy formulation for constrained and combined systems, *ASME Journal of Applied Mechanics* 63 (1996) 1004–1010.
[11] I. Fedotov, S. Joubert, J. Marais, M. Shatalov, Another approach to vibration analysis of stepped structures, *Electronic Transactions on Numerical Analysis (ETNA)* 24 (2006) 66–73.
[12] I. Fedotov, Y. Gai, A. Polyanin, M. Shatalov, Analysis for an N-stepped Rayleigh bar with sections of complex geometry, *Applied Mathematical Modelling* 32 (2008) 1–11.
[13] H. Li, B.J. Stone, Time domain modelling of a reciprocating engine, *Journal of Mechanical Systems and Signal Processing* 13 (1999) 169–178.
[14] A.G. Guzzomi, Torsional Vibration of Powertrains: An Investigation of Some Common Assumptions. Ph.D. Thesis, The University of Western Australia, 2007.
[15] B. Yang, Transfer functions of constrained/combined one-dimensional continuous dynamic systems, *Journal of Sound and Vibration* 156 (1992) 425–443.
[16] B. Yang, C.A. Tan, Transfer functions of one-dimensional distributed parameter systems, *ASME Journal of Applied Mechanics* 59 (1992) 1009–1014.
[17] B. Yang, H. Fang, Transfer function formulation of non-uniformly distributed parameter systems, *ASME Journal of Vibration and Acoustics* 116 (1994) 426–432.
[18] B. Yang, *Stress, Strain, and Structural Dynamics: An Interactive Handbook of Formulas, Solutions, and MATLAB Toolboxes*, Elsevier Science, Boston, 2005.
[19] C.T. Chen, *Linear Systems Theory and Design*, third ed., Oxford University Press, New York, 1999.
[20] P.M. Morse, H. Feshbach, *Methods of Theoretical Physics*, McGraw-Hill, New York, 1953.
[21] B. Yang, Integral formulas for non-self-adjoint distributed dynamic systems, *AIAA Journal* 34 (1996) 2132–2139.